

Electronic band structure of the buried SiO₂/SiC interface investigated by soft x-ray ARPES

J. Woerle,^{1,2} F. Bisti,¹ M.-A. Husanu,^{1,3} V. N. Strocov,^{1,a)} C. W. Schneider,¹ H. Sigg,¹ J. Gobrecht,¹ U. Grossner,² and M. Camarda¹

¹Paul Scherrer Institut, 5232 Villigen, Switzerland

²Advanced Power Semiconductor Laboratory, ETH Zurich, Physikstrasse 3, 8092 Zurich, Switzerland

³National Institute of Materials Physics, Atomistilor 105 bis, 077125 Bucharest-Magurele, Romania

(Received 12 January 2017; accepted 11 March 2017; published online 27 March 2017)

The electronic structure of the SiO₂/SiC (0001) interface, buried below SiO₂ layers with a thickness from 2 to 4 nm, was explored using soft X-ray angle-resolved photoemission spectroscopy with photon energies between 350 and 1000 eV. The measurements have detected the characteristic k-dispersive energy bands of bulk Silicon Carbide (SiC) below the SiO₂ layer without any sign of additional dispersive states, up to an estimated instrumental sensitivity of $\approx 5 \times 10^9 \text{ cm}^2 \text{ eV}$. This experimental result supports the physical picture that the large density of interface traps observed in macroscopic measurements results from dangling bonds randomized by the SiO₂ rather than from Shockley-Tamm surface derived states extending into the bulk SiC. *Published by AIP Publishing.*
[\[http://dx.doi.org/10.1063/1.4979102\]](http://dx.doi.org/10.1063/1.4979102)

The electronic structure of the SiO₂/SiC interface is of interest, among others, for its role in SiC MOSFETs. Although the quality of thermally grown oxides on SiC in terms of the breakdown electric field is comparable to that of SiO₂ grown on silicon,¹ the density of interface traps, D_{it} , is still more than one order of magnitude higher than that on Si. The reduction of the SiO₂/SiC interface defect density is necessary for MOSFET applications because they directly affect device performance degrading the channel mobility, altering the threshold voltage, and decreasing the reliability.

The exact origin of the high interface trap density of SiC is still not well understood. In the case of Si MOS structures, dangling bonds (DBs) at the interface are known to be the dominant defect structures.^{2,3} SiC has a higher surface density of atoms per unit area than Si but the density is not sufficient to justify the observed difference. It has also been observed that the D_{it} at the SiO₂/SiC(0001) interface is much higher than the ones of SiO₂/SiC(000-1) or SiO₂/SiC(11-20)^{2,3} under equivalent oxidation conditions and that this difference is found also in the case of deposited oxides (Si₃N₄, Al₂O₃, and AlN).⁴

The dependency of D_{it} on the crystallographic orientation could be either due to interface states derived from Shockley-Tamm (ST) surface states, which are intrinsically connected to the alteration of the $V(z)$ potential at the given crystal termination,⁵⁻⁷ or due to defects generated during the oxidation process, such as carbon by-products, the generation being crystallographic dependent.

However, although the role of residual carbon near the interface has been discussed extensively,^{8,9} a direct link between the carbon density near the interface and the interface state density has not been proven.

The ST-derived interface states would be deleterious as they would be intrinsically connected to the (0001) termination and thus independent of any treatment. This work aims

at investigating the nature of the D_{it} at the SiO₂/SiC(0001) interface by means of soft X-ray angle-resolved photoemission spectroscopy (SX-ARPES).

The samples used in this experiment were sections of 4° off (11-20) 4H SiC, 15 μm thick, n-type epitaxial layers (effective doping $4 \times 10^{15} \text{ cm}^{-3}$, as extracted by capacitance-voltage (CV) measurements) supplied by Cree. The samples were loaded into a furnace immediately after cleaning and were oxidized in pure O₂ at a temperature of 1050 °C in order to generate 2 nm and 4 nm thick SiO₂ layers (measured by X-ray reflectivity (XRR) and capacitance-voltage (CV) analysis of MOS devices). After oxidation, the SiO₂/SiC buried interface has been analyzed by means of SX-ARPES with photon energies around 1 keV and a beam spot size of 30 μm × 74 μm.

While the properties of clean SiC surfaces have already been investigated by means of angle-resolved photoelectron spectroscopy,^{10,11} this study explores the buried SiO₂/SiC interface by taking advantage of the significant increase of the photoelectron mean free path λ and thus the probing depth when using soft X-rays,¹² compensating for the decrease of the valence band photoexcitation cross-section with the high photon flux ($> 10^{13}$ photons/s/0.01%BW) of the ADDRESS beamline at the Swiss Light Source.¹³ A sketch of the SX-ARPES experimental geometry in relation to the Brillouin zone (BZ) of 4H-SiC is shown in Fig. 1.

The interpretation of the experimental data is based on the physical picture where the SiO₂/SiC (0001) interface states are closely related to the SiC (0001) surface states. Two types of states with different wave function characters can be distinguished in such a case: (1) interface states derived from dangling bonds (DBs) at the SiC surface and (2) interface states derived from ST states within the SiC which are intrinsic to the alteration of the $V(z)$ potential at the crystal termination.

The former situation is realized, for example, by DBs at the 2H-, 4H-, and 6H-SiC (0001) surfaces^{14,15} where the dangling bonds of the $(\sqrt{3} \times \sqrt{3})$ R30° reconstructed Si

^{a)}Electronic mail: vladimir.strocov@psi.ch

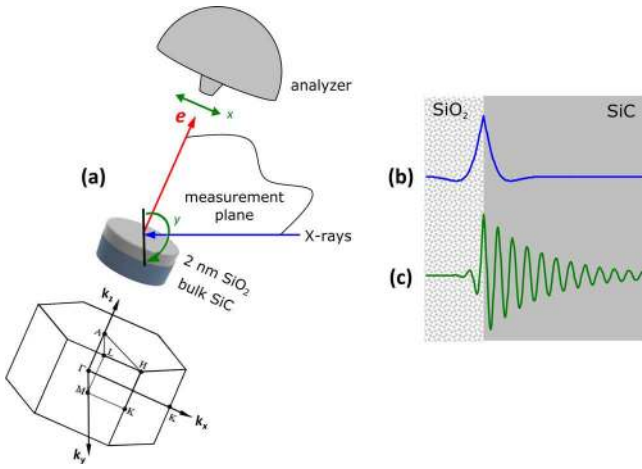


FIG. 1. (a) Experimental geometry relative to the BZ of 4H-SiC; (b) and (c) Schematic wave functions of the dangling bond (b) and Shockley-Tamm (c) derived interface states. The SX-ARPES experiment is most sensitive to the latter.

adatoms form the surface states D_{Si} dispersing in the surface-parallel momentum (k_x, k_y). Wave functions of the DB-derived interface states are typically aperiodic in the surface-perpendicular z-direction and sharply localized at the interface as shown in the sketch in Figure 1(b). In the case of this experiment, the growth of amorphous SiO_2 passivates and randomizes the DBs of the bare SiC surface to smear their energy levels and k-dispersions. Wave functions of the ST-derived interface states, on the other hand, will oscillate and extend into the SiC bulk typically over a few unit cells or more (see Figure 1(c)) similar to ST surface states on Al (100) (~ 5 nm)⁷ or topological surface states on Bi_2Se_3 (001) (~ 3 nm).¹⁶ Protected by the SiC bulk from their randomization by amorphous SiO_2 , the ST-derived interface states will show well-defined energies and band k-dispersions.¹⁴

The different character of the DB- and ST-derived SiO_2/SiC interface states will then determine the different photoemission (PE) response $\langle \Phi_f | \Phi_i \rangle$. At the high photon energies $h\nu$ used in SX-ARPES, the oscillation frequency of Φ_f increases proportionally to $\sqrt{h\nu}$ and its delocalization in the z-direction, determined by λ , increases to a few nm.

The aperiodic and strongly localized Φ_i of the DB-derived (defect) states dramatically reduces the $\langle \Phi_f | \Phi_i \rangle$ product and thus, at high energy, the photoemission response as compared to bulk SiC states (see, e.g., Ref. 17). Therefore, SX-ARPES is less sensitive to the DB-derived interface states. The ST-derived interface states, on the contrary, are

characterized by an oscillating Φ_i and extension into the bulk of the same order of the probing depth. Therefore, even at high energies, their $\langle \Phi_f | \Phi_i \rangle$ product, and thus high-energy photoemission response, is similar to those of the bulk SiC states. Related examples are Al (100) and Bi_2Se_3 (001) surface states^{7,16} which retain a significant photoemission response up to at least 1 keV, with the intensity oscillations as a function of $h\nu$ reflecting their Fourier composition. Hence, SX-ARPES is mostly sensitive to the ST-derived interface states with their sharp k-dispersions.^{6,7,16}

Figure 2 shows angle-integrated photoemission (PE) spectra of the Si 2p core levels, for the 4 nm thick oxide, measured through a series of increasing $h\nu$ as well as increasing photoelectron emission angle Θ relative to the surface normal. The spectra are acquired at p-polarization of the incident X-rays and aligned in binding energy E_B to compensate for sample charging depending on $h\nu$. The low- E_B peak is attributed to the Si atoms in SiO_2 and the high- E_B peak to SiO_2 . While the peak of crystalline SiC shows the characteristic Si 2p doublet with $2p_{1/2}$ and $2p_{3/2}$ components, this structure is smeared in SiO_2 because of its amorphous character. Most importantly, the Si-C peak, compared to the SiO_2 one, increases for increasing $h\nu$, i.e., for larger photoelectron mean free paths λ , and decreases for increasing grating angles Θ , i.e., in the case of higher surface sensitivities. This behaviour is consistent with a SiC substrate buried beneath a SiO_2 layer.

Figures 3(a) and 3(b) show raw ARPES intensity images $I(k_x, E_B)$ acquired at two different p-polarized photon energies $h\nu = 360$ and 826 eV, both corresponding to the same Γ -K direction in the bulk BZ of 4H-SiC. The surface-parallel momentum k_x is obtained from the photoelectron kinetic energy E_k and emission angle Θ as $k_x = 0.5124\sqrt{E_k} \sin \Theta - p_x$ where p_x corrects for the photon momentum $p = \frac{2\pi}{12.400} h\nu$ significant for the ADDRESS soft X-ray energies.¹⁸ The images are normalized to the angle dependent transmission of the ARPES analyzer as determined from the background intensity and are presented on a logarithmic scale. The k-dispersive spectral structure seen at $h\nu = 360$ eV indicates that coherent electrons excited in crystalline SiC can escape through the 2 nm-thick SiO_2 capping layer already at relatively small energies. The enhancement of the spectral contrast at 826 eV evidences the increase of the photoelectron mean free path λ with increasing energy, which is consistent with the core level data in Figure 2. Furthermore, the increase of λ sharpens the intrinsic k_z definition of the experiment¹⁹ which is evident as a smaller broadening of the \mathbf{k} -dispersion.

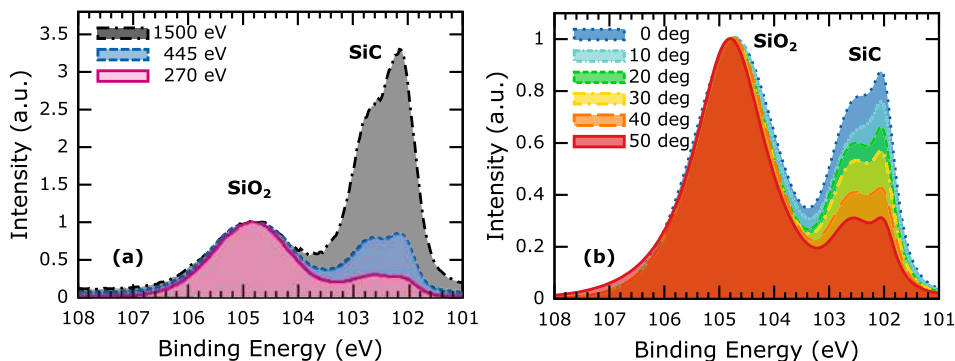


FIG. 2. Si 2p core levels measured under (a) increase of $h\nu$ at normal emission and (b) increase of Θ at $h\nu = 445$ eV. The SiC peak scales up compared to the SiO_2 one with $h\nu$ and scales down with Θ , which is consistent with SiC being buried below SiO_2 .

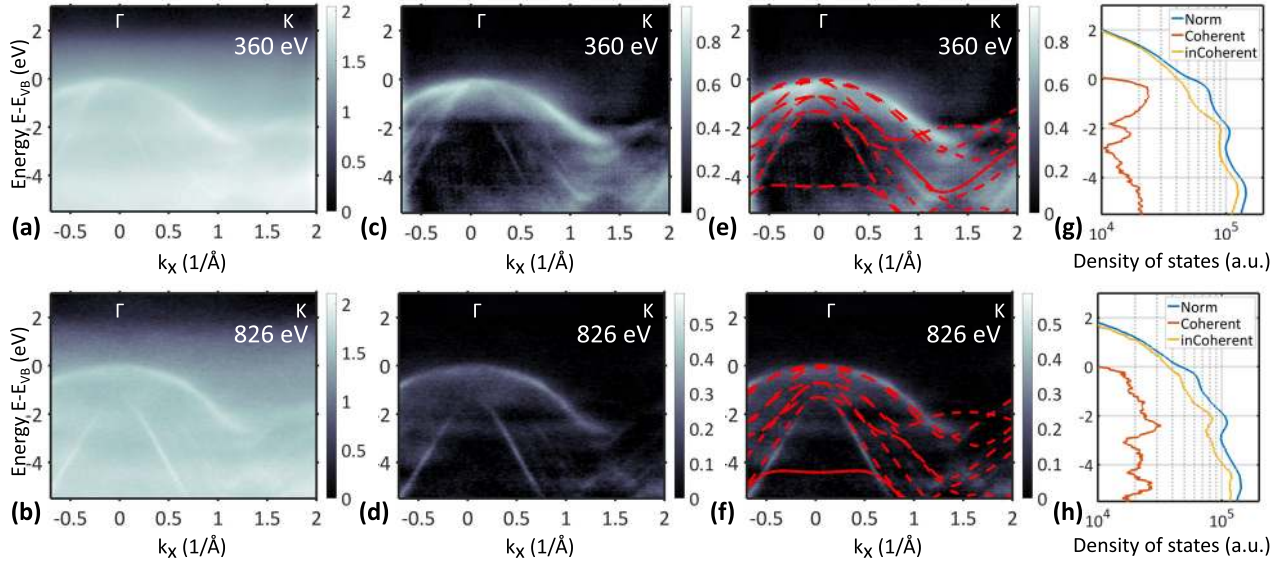


FIG. 3. Experimental valence band spectra of the SiO_2/SiC (0001) interface in the Γ -K azimuth compared with theory: (a) and (b) Images of the raw ARPES intensity measured with p-polarized incident X-rays and (c) and (d) angle-resolved coherent fraction of the ARPES images; (e) and (f) the same as (c) and (d) but with superimposed theoretical band structure of bulk SiC. (c) and (d) Γ -K angle-integrated total ARPES intensity decomposed in coherent and incoherent components. The two indicated photon energies correspond to the same Γ -K direction but with different probing depths.

The raw intensity is composed of (1) a sharp k-dispersive coherent component (I_{Co}) originating from the buried crystalline SiC and (2) a non-dispersive incoherent component (I_{inCo}). The latter is composed of a photoexcitation in the amorphous SiO_2 overlayer with a small admixture of the interface defect states and by photoelectrons excited in SiC and quasielastically scattered in SiO_2 on their escape to vacuum (the non-dispersive secondary electron contribution is relatively small). The total $I(k_x, E_B)$ can then be written as the sum of the coherent and incoherent contributions as

$$I(k_x, E_B) = I_{Co}(k_x, E_B) + I_{inCo}(E_B). \quad (1)$$

The incoherent contribution for each E_B value can be identified as the minimum of $I(k_x, E_B)$ over the whole k_x -range

$$I_{inCo}(E_B) = \min_{k_x} I(k_x, E_B), \quad (2)$$

which then yields I_{Co} simply as

$$\begin{aligned} I_{Co}(k_x, E_B) &= I(k_x, E_B) - I_{inCo}(E_B) \\ &= I(k_x, E_B) - \min_{k_x} I(k_x, E_B). \end{aligned} \quad (3)$$

The results of this decomposition procedure applied to the data are shown in Figure 3 as I in (a) and (b) and I_{Co} in (c) and (d). The I_{Co} spectral component can now be compared with the bulk band structure $E(k)$ ²⁰ of the 4H-SiC Γ -K direction in Figures 3(e) and 3(f). The latter was calculated in the framework of DFT using the Quantum Espresso software and ultra-soft pseudopotentials. The exchange and correlation terms are described using the GGA approximation. A 30 Ry cutoff for the plane wave expansion and a 400 Ry cutoff for the charge density integration have been employed with a $5 \times 5 \times 2$ k-mesh sampling for the coordinate relaxation and a denser grid of $10 \times 10 \times 3$ for the band structure calculation. The comparison demonstrates that the coherent

ARPES response of the SiO_2/SiC (0001) interface is formed exclusively by the bulk band structure of 4H-SiC and with both coherent and incoherent components decreasing below noise level at ~ 2 eV above the SiC valence band (see Figures 3(g) and 3(h)). At the two considered photon energies, no additional k-dispersive spectral structures, in the band gap of SiC or within its valence band, are detected which would be indicative of ST-derived interface states.

In search for potential ST-derived interface states, the measurements have been extended to the opposite s-polarization of incident X-rays (to check against silenced combinations of the X-ray polarization and initial state symmetry) and to a wide $h\nu$ range between 400 and 1500 eV (to check against silenced combinations of X-ray photon energies and k vector, where the final-state Φ_f becomes essentially anti-phase to the Fourier component of the initial-state Φ_i and quenches the matrix element $\langle \Phi_f | \Phi_i \rangle$ ^{5,6}). In all measurements, no trace of k-dispersions indicative of the ST-derived states could be found neither in the gap nor in the valence band region of SiC (see [supplementary material](#)).

This study has also been extended to other regions of the k-space. For this purpose, the ARPES intensity at $h\nu = 570$ eV has been measured, bringing k_z to the same Γ -K-M plane as in Figure 3, i.e., as a function of two-dimensional momenta (k_x, k_y). Figure 4 represents the experimental $I(k_x, k_y)$ as its isoenergetic cuts for a series of E_B through the valence band compared with the corresponding calculations. Although in the band gap region only a homogeneous intensity can be seen (not shown here), the cuts of the valence bands appear in excellent agreement with theory again without any trace of additional k-dispersive interface states. ARPES analysis along the Γ -K direction (the same as Figure 3) performed on the 4 nm thick oxide sample showed essentially identical spectra, except for a smaller amplitude of the coherent SiC signal.

All SX-ARPES measurements confirm the absence of ST-derived interface states at the SiO_2/SiC interface. The detection

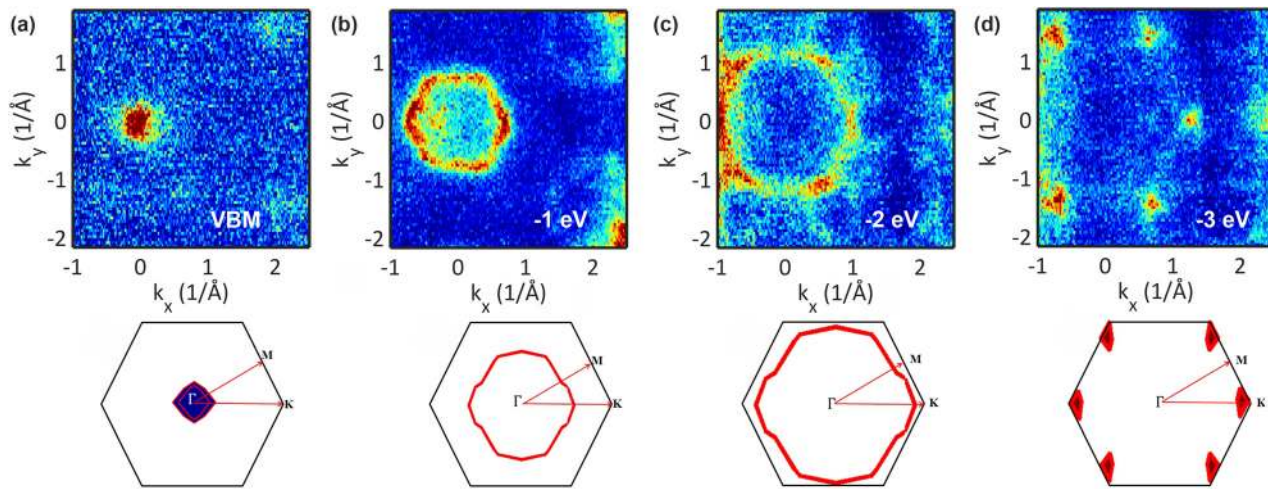


FIG. 4. Fermi surfaces (Γ -K, LV polarization, and $h\nu = 570$ eV) which are also represented in Fig. 2 as constant- E_B maps (CEMs) of PE intensity $I(k_x, k_y)$ for different E_B values. Shown CEM contours are centered at the VBM and $E_B = 1, 2$ and 3 eV below the VBM.

limit of the experiment, taking into account the effective density of states in the valence band N_v at $T = 11$ K, assuming an initial and final state extension of 1 nm, 5% signal-to-noise minimum detection level and an energy resolution of 100 meV, can be estimated around $\sim 5 \times 10^9$ $\text{cm}^{-2} \text{eV}^{-1}$. This value falls into the same sensitivity range of conductance-voltage (GV) measurements.⁴ The absence of the ST-derived interface states supports the high technological promise of the SiO_2/SiC interface. Indeed, although dangling bonds and defect states can in principle be quenched by proper cleaning,²¹ oxidation processes,²² or passivation of the dangling bonds,²³ the ST-derived interface states extending to SiC would be less sensitive to any surface treatments. Furthermore, the narrow interface localization of the DB-derived and defect interface states shrinks their overlap with the bulk-derived SiC wave functions responsible for electron transport near the interface and renders them less important for incoherent scattering and thus trapping activity against the interface charge carriers.

See [supplementary material](#) for additional SX-ARPES spectra of the SiO_2/SiC (0001) interface along Γ -K taken at different photon energies.

We thank E. E. Krasovskii for expert advice. F. Bisti acknowledges funding by the Swiss National Science Foundation Grant No. 200021_146890 and by the European Community's Seventh Framework Programme (FP7/2007-2013) Grant No. 290605 (PSI-FELLOW/COFUND). M.-A. Husanu was supported by the Swiss Excellence Scholarship Grant ESKAS-No. 2015.0257. J. Woerle and M. Camarda were supported by the National Research Programme *Energy Turnaround* (NRP 70) of the Swiss National Science Foundation (SNSF).

¹E. Nicollian and J. Brews, *MOS Physics and Technology* (Wiley-Interscience, 1982).

²P. Friedrichs, E. P. Burte, and R. Schorner, "Dielectric strength of thermal oxides on 6H-SiC and 4H-SiC," *Appl. Phys. Lett.* **65**, 1665 (1994).

³K. Fukuda, M. Kato, K. Kojima, and J. Senzaki, "Effect of gate oxidation method on electrical properties of metal-oxide-semiconductor field-effect

transistors fabricated on 4H-SiC C(0001) face," *Appl. Phys. Lett.* **84**, 2088 (2004).

⁴T. Kimoto and J. Cooper, *Fundamentals of Silicon Carbide Technology* (Wiley, 2014).

⁵S. G. Louie, P. Thiry, R. Pinchaux, Y. Pétrouff, D. Chandresris, and J. Lecante, "Periodic oscillations of the frequency-dependent photoelectric cross sections of surface states: Theory and experiment," *Phys. Rev. Lett.* **44**, 549–553 (1980).

⁶E. E. Krasovskii and W. Schattke, "Angle-resolved photoemission from surface states," *Phys. Rev. Lett.* **93**, 027601 (2004).

⁷P. Hofmann, C. Søndergaard, S. Agergaard, S. V. Hoffmann, J. E. Gayone, G. Zampieri, S. Lizzit, and A. Baraldi, "Unexpected surface sensitivity at high energies in angle-resolved photoemission," *Phys. Rev. B* **66**, 245422 (2002).

⁸V. V. Afanas'ev, M. Bassler, G. Pensl, and M. J. Schulz, "Intrinsic SiC/SiO₂ interface states," *Phys. Status Solidi A* **162**, 321 (1997).

⁹M. Bassler, G. Pensl, and V. V. Afanas'ev, "'Carbon cluster model' for electronic states at SiC/SiO₂ interface," *Diamond Relat. Mater.* **6**, 1472 (1997).

¹⁰K. V. Emtsev, T. Seyller, L. Ley, A. Tadich, L. Broekman, J. Riley, R. Leckey, and M. Preuss, "Electronic properties of clean unreconstructed 6H-SiC(0001) surfaces studied by angle resolved photoelectron spectroscopy," *Surf. Sci.* **600**, 3845–3850 (2006).

¹¹C. Virojanadara, M. Hetzel, L. Johansson, W. Choyke, and U. Starke, "Electronic and atomic structure of the 4H-SiC (1-102)-c(2x2) surface," *Surf. Sci.* **602**, 525–533 (2008).

¹²C. Powell, A. Jablonski, I. Tilinin, S. Tanuma, and D. Penn, "Surface sensitivity of Auger-electron spectroscopy and X-ray photoelectron spectroscopy," *J. Electron Spectrosc. Relat. Phenom.* **98–99**, 1–15 (1999).

¹³V. Strocov, T. Schmitt, U. Flechsig, A. Imhof, Q. Chen, J. Raabe, R. Betemps, D. Zimoch, J. Krempasky, X. Wang, M. Gironi, A. Piazzalunga, and L. Patthey, "High-resolution soft x-ray beamline ADDRESS at the Swiss Light Source for resonant inelastic X-ray scattering and angle-resolved photoelectron spectroscopies," *J. Synchrotron Radiat.* **17**, 631–643 (2010).

¹⁴J. Soltys, J. Piechota, M. Łopuszynski, and S. Krukowski, "A comparative DFT study of electronic properties of 2H-, 4H- and 6H- SiC(0001) and SiC(000-1) clean surfaces: significance of the surface Stark effect," *New J. Phys.* **12**, 043024 (2010).

¹⁵T. Seyller, K. V. Emtsev, R. Graupner, and L. Ley, "Initial stages of thermal oxidation of 4H-SiC (11–20) studied by photoelectron spectroscopy," *Mater. Sci. Forum* **457–460**, 1317–1320 (2004).

¹⁶R. Queiroz, G. Landolt, S. Muff, B. Slomski, T. Schmitt, V. N. Strocov, J. Mi, B. Iversen, P. Hofmann, J. Osterwalder, A. Schnyder, and J. Dil, "Sputtering-induced reemergence of the topological surface state in Bi₂Se₃," *Phys. Rev. B* **93**, 165409 (2016).

¹⁷E. Razzoli, M. Kobayashi, V. N. Strocov, B. Delley, Z. Bukowski, J. Karpinski, N. C. Plumb, M. Radovic, J. Chang, T. Schmitt, L. Patthey, J. Mesot, and M. Shi, "Bulk electronic structure of superconducting LaRu₂P₂ single crystals measured by soft-X-ray angle-resolved photoemission spectroscopy," *Phys. Rev. Lett.* **108**, 257005 (2012).

- ¹⁸V. N. Strocov, X. Wang, M. Shi, M. Kobayashi, J. Krempasky, C. Hess, T. Schmitt, and L. Patthey, "Soft-X-ray ARPES facility at the ADDRESS beamline of the SLS: Concepts, technical realisation and scientific applications," *J. Synchrotron Radiat.* **21**, 32–44 (2014).
- ¹⁹V. N. Strocov, "Intrinsic accuracy in 3-dimensional photoemission band mapping," *J. Electron Spectrosc. Relat. Phenom.* **130**, 65–78 (2003).
- ²⁰H.-G. Junginger and W. van Haeringen, "Energy band structures of four polytypes of Silicon Carbide calculated with the empirical pseudopotential method," *Phys. Status Solidi* **37**, 709 (1970).
- ²¹V. V. Afanas'ev, A. Stesmans, M. Bassler, G. Pensl, M. J. Schulz, and C. I. Harris, "Elimination of SiC/SiO₂ interface states by preoxidation ultraviolet-ozone cleaning," *Appl. Phys. Lett.* **68**, 2141 (1996).
- ²²K. Kita, R. Kikuchi, H. Hirai, and Y. Fujino, "Control of 4H-SiC (0001) thermal oxidation process for reduction of interface state density," *ECS Trans.* **64**, 23 (2014).
- ²³G. Y. Chung, C. C. Tin, J. R. Williams, K. McDonald, M. Di Ventra, S. T. Pantelides, and L. Feldman, "Effect of nitric oxide annealing on the interface trap densities near the band edges in the 4H polytype of silicon carbide," *Appl. Phys. Lett.* **76**, 1713 (2000).